Photodegradation of Ciprofloxacin and its interaction with Cu(II) in different water matrices: insight into degradation pathways

Fang Zhong, Wenyu Huang, Xiaoqing Feng, Jia Zhang, Hongrui Zhang, Yiwu Dong, Jingrao Li, Liang Zou, Feishu Cao, Gilles Mailhot

Photodegradation of Ciprofloxacin and its interaction with Cu(II) in different water matrix: insight into degradation pathways

Fang Zhong [a], Wenyu Huang [a b *], Xiaoqing Feng [a b], Jia Zhang [a], Hongrui Zhang [a], Yiwu Dong [a], Jingrao Li [a], Liang Zou [b], Feishu Cao [c], Gilles MAILHOT [d]

[a] School of Resources, Environment and Materials, Guangxi University, Nanning 530004, China

[b] Guangxi Bohuan Environmental Consulting Services CO.,LTD, Nanning 530000, China

[c] Guangxi Key Laboratory of Environmental Pollution Control and Ecological Restoration Technology, Nanning 530000, China

[d] Université Clermont Auvergne, CNRS, Clermont Auvergne INP, Institut de Chimie de Clermont-Ferrand, F-63000 Clermont‑Ferrand, France

***Corresponding Author:**

Wenyu Huang, Ph.D

School of Resources, Environment and Materials of Guangxi University, Nanning, 530004, P.R.China

Guangxi Bohuan Environmental Consulting Services CO.,LTD, Nanning 530000, China

Email: huangwenyu@gxu.edu.cn

Highlights

- The effect of Cu(II) on CIP degradation efficiency varies greatly in different water matrixs.
- The water matrix and Cu(II) can change the main reactive oxygen species in the CIP degradation system.
- Cu(II) changes the reaction site of CIP, leading to the formation of hydroxylation, nitrification and cyclopropyl group cleavage on products.
- Cu(II) and water matrix increase the toxicity of CIP products by changing the original products.

ABSTRACT

Co-contamination of ciprofloxacin and Cu(II) is common in marine aquaculture water. However, people often ignore the transmission and transformation of the two in natural water matrices. This study sought to determine the impact of Cu(II) on the ciprofloxacin (CIP) degradation process in distilled (DI) and simulated (SI) mariculture water, as well as to develop a relationship between Cu(II), CIP, and the products of its degradation. Firstly, the use of complexation assays and analog computations revealed that Cu (II) can form complexes by binding to the O of the carbonyl group (C=O) and O of the carboxyl group (COOH) in the CIP molecule. Secondly, photodegradation experiments showed that Cu(II) significantly hindered the degradation effect of CIP in DI water, while Cu(II) did not significantly hinder the degradation of CIP in SI water. In addition, the effect of Cu(II) on the degradation mechanism of CIP was determined by combining quenching and EPR experiments, Materials Studio software calculations, and UPLC-MS results. It was demonstrated that Cu(II) enhanced the production of singlet oxygen ($^1O_2$), hydroxyl radicals (•OH), and superoxide radicals ($•O_2^-$) in DI water. In the presence of Cu(II), CIP undergoes hydroxylation and decarbonylation reactions to form hydroxylated and nitroxylated products in addition to direct defluorination and piperazine ring cleavage, which are then followed by complexation reactions with Cu(II). However, in SI water, the production of $^1O_2$ depends on the indirect action of Cu(II) and the excited state transformation of organic matter. Experimental evidence has shown that CIP can create intermediate compounds that include O-O peroxide rings, with or without the presence of Cu(II). When Cu(II) is present, the cyclopropyl group of the CIP molecule is more prone to transformation and so degradation. Finally, the toxicity assessment results showed that both Cu(II) and SI water increased the toxicity of the products.

Keywords: Ciprofloxacin; Photodegradation; Simulated mariculture water; Cu(II); Degradation mechanism

1 Introduction

Ciprofloxacin (CIP) is a second-generation fluoroquinolone antibiotic that is widely utilized in medicines, aquaculture, and agriculture because of its antibacterial action against Staphylococci(Guo et al., 2023). However, CIP, like other antibiotics, cannot be entirely metabolized by the human body or degraded in nature, thus it penetrates rivers, sediments, and agricultural soils as parent compounds, conjugates, and intermediates(Schwarzenbach et al., 2006; Tong et al., 2011). Even low concentrations of CIP in aquatic environments can endanger ecosystems, human health, and biological wastewater treatment processes(Bel,

2009; Guo et al., 2024). As a result, it is critical to investigate the fate and behavior of CIP in aquatic systems.

The main chain of CIP is 4-oxo-1,4-dihydroquinoline, which contains a fluorine atom and a piperazine ring, which can significantly enhance its photolysis(Deng et al., 2022; Tan et al., 2018). Therefore, photocatalytic technology(Muthukumar, 2024; Van Doorslaer, 2011; Yu et al., 2021) and photolysis technology(Lulijwa et al., 2020; Qin et al., 2018; Silva et al., 2021; Wu et al., 2018) are often used for the degradation of CIP. However, photocatalytic technology is usually inseparable from the preparation of photocatalysts. Currently, most catalyst research focuses on laboratory conditions and cannot be directly applied to actual water environments. Therefore, photodegradation is a more effective and easy-to-operate treatment method. However, most antibiotics, including CIP, do not exist alone or in isolation in the actual water matrix and usually coexist with organic matter and various inorganic ions. Therefore, it is necessary to study the photolysis behavior of CIP in complex water matrix.

Organic matter absorbs photons and transitions to the excited triplet state, producing more reactive oxygen species (ROS) under the combined action of water and molecular oxygen, further oxidizing pollutants. It has been reported that terrestrial humus components in natural colloidal particles (NCP) can significantly promote the photodegradation of CIP, and their contribution to indirect photolysis is close to 46%(Cheng et al., 2021). It can be seen that organic matter in water bodies will significantly affect the photodegradation pathway of CIP. It is worth noting that there are significant differences in the effects of humus on CIP photodegradation under different experimental conditions. In laboratory pure water, only humic acid at higher concentrations has a slight promoting effect on the photodegradation of CIP(Rodríguez-López et al., 2021). Ciprofloxacin in ice is significantly affected by changes in the concentration of fulvic acid (FA). When $C_{FA}/C_{CIP} \leq 60$, it exhibits a promoting effect; when $C_{FA}/C_{CIP} \geq 60$, it exhibits an inhibitory effect(Li et al., 2022). It is not difficult to find that the current research perspective is mainly focused on the impact of organic matter on the photolysis of single antibiotics, while the photolysis behavior and environmental hazards of combined pollution of heavy metals and antibiotics in actual water matrices are not well understood.

On the other hand, the coexistence of metal ions and antibiotics is also a common example. Metal ions can affect the photolysis process of antibiotics through various pathways(Khurana et al., 2021; Ramotowska

et al., 2020; Q. Wang et al., 2022). It is worth noting that Cu(II) is often added as a growth promoter for marine aquaculture animals, and the average concentration in aquaculture tailwater exceeds the Class I marine sediment quality standard, which has attracted widespread attention from scholars(Fan et al., 2022). In current reports, Cu(II) exhibits completely different effects on different antibiotics. For example, Cu(II) can form a complex with tetracycline, reducing molecular stability and making it more susceptible to ROS attack, thereby promoting the degradation of TC. In addition, when Cu(II) coexists with tetracycline, ligand-metal charge transfer (LMCT) is more likely to occur, and the Cu(II)/Cu(I) cycle induces more singlet oxygen ($^1O_2$) and hydroxyl radicals (•OH) to participate in the degradation of TC(Xu et al., 2023). However, the complexation effect between sulfamethoxazole (SMZ) and Cu(II) will significantly inhibit the photoreactivity of SMZ, thereby severely inhibiting the degradation of SMZ(Sha et al., 2022). Although there are more and more studies on the role of Cu(II) in the environmental behavior of antibiotics, there is still a lack of research on the photolysis process of fluoroquinolone antibiotics represented by ciprofloxacin and Cu(II) combined pollution in water environments.

The main objective of this study was to investigate the effect of Cu(II) on the photochemical fate of CIP in deionized and SI water. Initially, the complexation ratio between CIP and Cu(II) was established, and the specific location of the complexation between the two substances was calculated and analyzed using Raman characterization and Materials Studio software. Afterward, we conducted a detailed discussion on the factors affecting the degradation rate of Cu(II) and CIP in different water matrices. The degradation sites and pathways were determined by performing active ingredient quenching experiments, EPR spectroscopy, DFT calculations, and MS analysis. An in-depth analysis was performed to examine the changes in the degradation mechanism of CIP in the presence of Cu(II) in different water matrices. Finally, the toxicity of CIP and its byproducts was analyzed using toxicity assessment software. This study provides a new perspective on the fate of combined pollution in aquatic environments.

2 Materials and methods

2.1 Reagents

Ciprofloxacin (>98.0%), triethylene diamine and Sorbic acid (HAD) were provided by Shanghai Macklin Biochemical Co. LTD. Copper chloride dehydrate, calcium chloride anhydrous, potassium chloride, ammonia chloride, sodium sulfate anhydrous, sodium chloride glucose, magnesium sulfate heptahydrate,

isopropanol, chloroform and citric acid monohydrate were obtained from Guangdong Guanghua Science and Technology Co. LTD. Sodium nitrate, sodium bicarbonate, sodium nitrite, potassium dihydrogen phosphate, potassium bromate and sodium bromide were supplied by Chengdu Jinshan Chemical Reagent Co. LTD. Humic acid was purchased from Sigma. Phosphoric acid and acetonitrile were of high-performance liquid chromatography (HPLC) grade (≥99.9%) and were purchased from MERCK.

Stock solutions of 200 μmol L^{-1} of CIP and 0.025 mol L^{-1} of $CuCl_2$ were prepared in DI water, stored in the dark at 4 ℃, and used within one week. The pH of all solutions was adjusted with HCl/NaOH to circumvent any potential effects that the buffer might have had. The chemicals were of analytical grade and were used without further purification. Distilled (DI) water was used in all experiments. The composition and content of the simulated (SI) mariculture water are presented in **Table S1**.

2.1.1 Complex preparation between CIP and Cu(II)

A 100 mL glass tube was used as the reaction vessel, and 50 mL of reaction solution was added in each experiment. The initial concentration of CIP was 0.01 mmol L^{-1}, and the amount of Cu(II) added was CIP: Cu(II) molar ratio of 1:0, 1:0.5, 1:1, 1:1.5, and 1:2, respectively. The pH of the solution was adjusted to 7 and then the solution was stirred with a magnetic stirrer for 30 min. These solutions were analyzed by UV-Visible Spectrophotometer.

In addition, the composite solution was refrigerated at 4 °C for 24 h to ensure that the CIP and Cu(II) were fully complexed, then the solution was removed and the blue crystals formed were filtered and dried to constant weight. The resulting blue crystals were ground into powder to measure Raman spectra.

2.1.2 Photodegradation Experiments

Photodegradation experiments were carried out in a photoreactor with a 350 W xenon lamp, which was used to simulate sunlight. A quartz tube with a capacity of 250 mL was utilized as the reaction vessel, and 100 mL of the reaction solution was introduced in each experimental. A certain amount of CIP and $CuCl_2$ stock solutions were pipetted separately and mixed, and the pH of the solution was adjusted with NaOH/HCl. The solutions were then placed in the reactor and the magnetic stirrer was switched on for 30 min, after which the temperature controlled water circulation and xenon lamps were switched on successively to maintain the temperature of the irradiated solutions at a fixed temperature (293 ± 2 K). Finally, samples were

taken at fixed time intervals, passed through a 0.22 μm organic-based filter membrane, and the concentration of the substance was determined by ultra-performance liquid chromatography (UPLC). The removal efficiency of CIP after the photodegradation were calculated from the following equation:

$$R = \frac{C_0 - C_t}{C_0} \times 100\% \#(1)$$

where R, C_0, and C_t represent the removal efficiency, the concentrations of CIP at the initial moment and time t, respectively.

Quenching experiments were used to determine the contribution of active species during CIP photodegradation. Isopropyl alcohol (IPA), triethylenediamine (DABCO), chloroform (Chlor) and potassium bromate ($KBrO_3$) were used to quench •OH, $^1O_2$, $•O_2^-$, and e^-, respectively.

2.1.3 Analytical methods

Ultra-performance liquid chromatography (UPLC H-CLASS Waters, America) was employed to ascertain the CIP concentration in the aqueous solution. The specific detection conditions are as follows: the mobile phase consists of 0.025% phosphoric acid and acetonitrile (V1:V2=87:13) with a flow rate of 0.35 $mL \cdot min^{-1}$, the detection wavelength is set at λ=275 nm, the injection volume was 5 μL, and the running time lasted for 3 min and the column was maintained at a temperature 40 ℃.

Characterization of complexes was determined by Via Reflex laser Raman spectrometer and UV-2550 UV-Visible Spectrophotometer. Active oxidants were captured by DMPO or TEMP and identified by electron paramagnetic resonance (EPR, Bruker A300, GER). The characterization of the excited states of CIP: Cu(II) at different ratios was conducted using the FL3C-111 TCSPC high-sensitivity steady-state-transient fluorescence spectrometer. The products were analyzed using a Waters Xevo G2QTOF ultra-high-performance liquid phase mass spectrometer (UPLC-MS)(**Text S1**).

2.1.4 Theoretical calculation

The active sites within the molecules were analyzed using the Materials Studio software. The $DMol_3$ module is used to simulate the frontier orbital, which is based on density functional theory (DFT)(Delley, 2000). The local density approximation- Perdew Wang 19 (LDA-PWC) functional was chosen as the exchange correlation in the simulated process. Calculation parameters are as follows: convergence tolerance energy, max force, max displacement and self-consistent field (SCF) tolerance were set to 2.0×10^{-5} Ha, 0.004 Ha/Å, 0.005 Å, 1.0×10^{-5} eV/atom, respectively. All electron and doubled numerical basis sets with

d-polarization functions (DND) were chosen as core treatment and atomic orbital basis sets, respectively.

2.1.5 Toxicity evaluation

Based on the quantitative structure-activity relationship (QSAR) model, the toxicity estimation software tool (T.E.S.T. v. 5.1.2.0) and the ecological structure-activity relationship model (ECOSAR. v. 2.2) software were used to calculate and evaluate the toxicity and potential risks of the intermediates of ciprofloxacin(Yang, 2021; Liu et al., 2024). T.E.S.T is mainly used to predict the bioaccumulation factor, developmental toxicity, and mutagenicity indicators of the intermediates. In addition, ECOSAR is used to estimate the acute and chronic toxicity levels of various aquatic organisms, including the median lethal concentration (LC_{50}) of fish, Daphnia (LC_{50}), and the concentration of 50% maximum effect (EC_{50}) of green algae.

3 Results and discussion

3.1 Investigation of complexation between Cu(II) and CIP

The solutions containing various ratios of CIP and Cu(II) were analyzed using a UV-Vis spectrophotometer (**Fig. 1a**). The maximum absorption wavelength showed redshifts and the absorption intensity increased after the addition of Cu(II), indicating interaction between Cu(II) and CIP. Furthermore, the absorbance reached maximum when the complexation ratio of CIP and Cu(II) was 1:1, indicating that CIP and Cu(II) formed a complex in a 1:1 ratio. This analysis confirms the existence of a complexation reaction between CIP and Cu(II).

To further confirm the complexation site between CIP and Cu(II), laser Raman spectrometer was used to characterize CIP and Cu(II)-CIP complex, sample obtained after precipitation at 4°C (**Fig. 1b**). The results showed that the carbonyl (C=O) peak near 1614 cm^{-1} and the antisymmetric carboxyl (O-C=O) peaks at 1590 cm^{-1} and 1380 cm^{-1} were all weakened or disappeared. Based on this, it can be concluded that Cu(II) forms a complex with the CIP molecule through the O atom of the carboxyl (COOH) in the CIP molecule and the O atom of the carbonyl (C=O) in the keto group (**Fig. S1**). In general, the structure of CIP comprises nitrogen (N) and oxygen (O) atoms that would provide lone pair electrons to interact with Cu(II)(Di Wu, 2012). Subsequently, the highest occupied molecular orbital (HOMO) and lowest unoccupied molecular orbital (LUMO) of the N and O atoms in the CIP molecule and Cu(II) in $CuCl_2$ were calculated individually by Materials Studio software (**Table S2**). The calculations indicate a strong interaction between the O atoms

of the CIP molecule and Cu(II), which further validates the Raman results. The O atoms of C=O and O-C=O will serve as complexing sites for CIP and Cu(II).

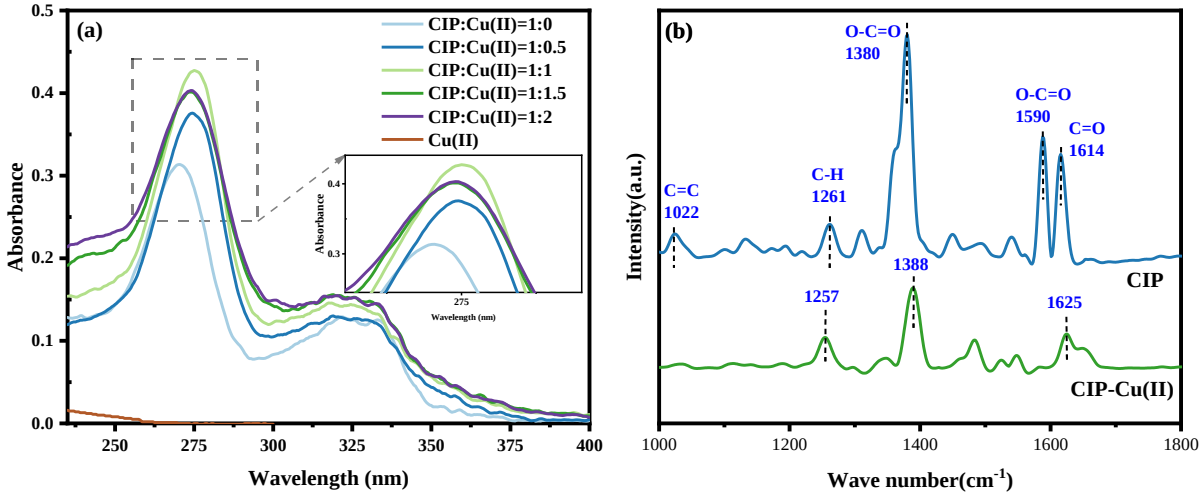

Fig. 1. (a) UV-Visible spectra of solutions with different CIP and Cu(II) ratios. The reaction conditions: [CIP]=0.01 mM, [Cu(II)] from 0 to 0.02 mM pH=7; (b) Laser Raman spectra of CIP and CIP-Cu(II) compound.

3.2 Effect of Cu (II) on CIP degradation

Cu(II) concentrations in simulated (SI) mariculture water are significantly higher than those in CIP(Wei et al., 2015), which may affect the UV-visible spectrum and accelerate the photodegradation process. The absorption spectra and the quantity of the free Cu(II) in the water demonstrated that the absorption in the system reached a maximum and the concentration of Cu(II) was minimal at a Cu(II) concentration of 0.4 mmol L^{-1} and a CIP concentration of 10 μmol L^{-1} (**Fig. S2** and **Table S3**). As a result, the concentration ratio of CIP: Cu(Ⅱ)=10 μmol L^{-1}: 0.4 mmol L^{-1} was employed in the subsequent experiments.

The impact of Cu(II) on the photodegradation efficiency of CIP in DI water and SI water is presented in **Fig. 2**. It is clear that the addition of Cu (II) can substantially diminish the CIP degradation in both systems. Cu(II) complexes with CIP, enhancing the stability of the molecular structure and reducing its reactivity which leads to a decrease in the photodegradation efficiency(Duong et al., 2008). Furthermore, the free Cu(II) in the solution can form additional complexes with the byproducts of photodegradation, which could potentially interfere with photon absorption and hinder the photodegradation process of CIP. However, as the length of irradiation increased, the degradation progressed gradually and the final degradation efficiency did

not vary significantly.

Fig. 2 shows that Cu(II) has an impact on the photodegradation of CIP in DI and SI water matrix. The efficiency of CIP photodegradation in SI water was lower than those in DI water. The lower photodegradation efficiency of CIP in SI water could be preliminarily attributed to the presence of coexisting substances, such as organic matter and inorganic ions. These components may either produce reactive oxygen species (ROS) through photolysis or shield/quench the ROS. We have formulated the following rationale based on comparative testing (**Fig. S3**). The complexation constants of Ca(II)-CIP and Cu(II)-CIP in SI water were 11.3 and 14.7, respectively. This suggests that metal ions have a competitive connection with each other, which has an impact on the degradation of CIP (**Fig. S3a**)(Chen et al., 2013; Cuprys et al., 2018). The hydrolysis of NH_4^+ in solution with OH^- increases the H^+ concentration in solution and decreases the yields of •OH and e^-, thereby inhibiting the degradation efficiency of the CIP-Cu(II) composite system. Nevertheless, the hydrolysis of NH_4^+ is a reversible reaction, resulting in an unstable H^+ concentration in solution. As a result, the suppression of this reaction is also not stable(He et al., 2011). Furthermore, the water contains both humic acid (HA) and fulvic acid (FA) as metal complexing agents. These agents can form a robust complex with Cu(II) (the complexation constants of HA-Cu(II) were 9.26 and FA-Cu(II) were 8.58), then attenuates the inhibitory effects of metal ions(**Fig. S3b**)(Chiron et al., 2006; Garbin et al., 2007; Yang and van den Berg, 2009). Furthermore, organic acids also can create excited states in the water, leading to the formation of $^1O_2$ and promoting the photolysis of CIP(Monti et al., 2001). On the other hand, anions present in water (e.g. SO_4^{2-}, NO_3^-, Cl^-, Br^-) can suppress ROS in solution and simultaneously interfere with the absorption of light by CIP (Eqs. (2)~(5)) (**Fig. S3c**)(Chang et al., 2014; Ge et al., 2010; Hu et al., 2019). However, the photodegradation of antibiotics by NO_3^- has a twofold impact, as it can either absorb photons and produce ROS, promoting photolysis, or react to generate NO_2^-, NO_3^{2-}, and OH^-, which impedes photolysis (Eqs. (S1)~(S6))(Ge et al., 2010; Trovó et al., 2009; Wolters and Steffens, 2005). As a result, the degradation rate and efficiency of CIP in the SI water were inhibited compared to DI water, but the inhibition was not significant. Additionally, the degradation rate of CIP in SI water was slightly faster than that in DI water in the presence of humic acid and Cu(II).

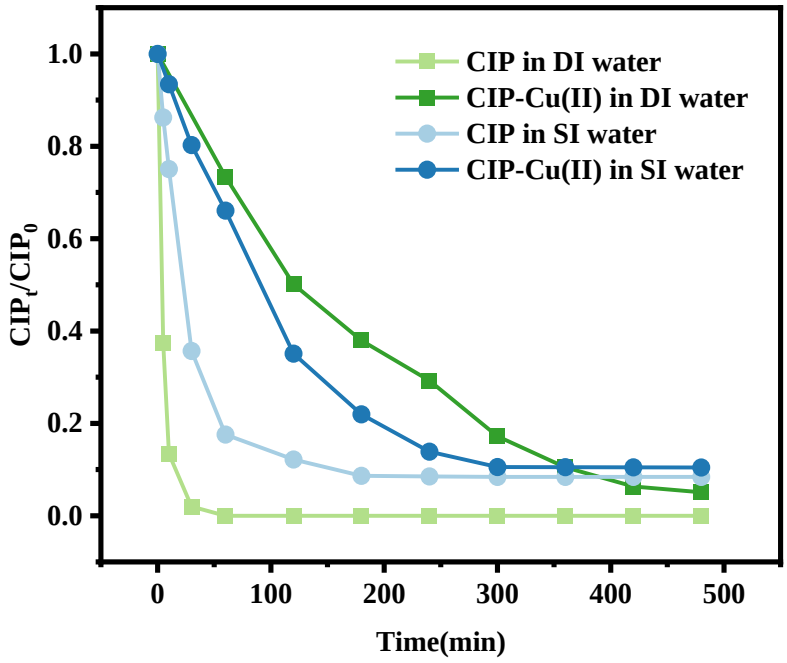

Fig. 2. Photodegradation in four different systems. The reaction conditions: the molar ratio of CIP: Cu(II)= 1:40, $[CIP]_0$=0.01 mM, $[Cu(II)]_0$ = 0.4 mM, pH=7.

Equations

$$SO_4^{2-} + \bullet OH \rightarrow SO_4^{\bullet -} + OH^- \qquad k = 1.5 \times 10^6\ L(mol \cdot s)^{-1} \#(2)$$

$$Cl^- + \bullet OH \rightarrow ClOH^{\bullet -} \qquad k = 4.3 \times 10^9\ L(mol \cdot s)^{-1} \#(3)$$

$$Br^- + \bullet OH \rightarrow BrOH^{\bullet -} \qquad k = 1.1 \times 10^{10}\ L(mol \cdot s)^{-1}\ \#(4)$$

$$NO_3^- + \bullet OH \longrightarrow NO_3^{\bullet -} + OH^- \qquad k = 1.0 \times 10^{10}\ L(mol \cdot s)^{-1} \#(5)$$

3.3 Effect of Cu(II) on the photodegradation mechanism of CIP under different aqueous media

3.3.1 Photodegradation pathway in distilled water

CIP typically undergoes direct and indirect photolysis. For direct photolysis, CIP leads to the formation of a triplet excited state ($^3CIP^*$), whereby it absorbs photons and subsequently undergoes a further chemical breakdown under the influence of light(Monti et al., 2001; A. Wang et al., 2022). For indirect photolysis, CIP receives photons, thereby forming a triple excited state of CIP ($^3CIP^*$). Subsequently, $^3CIP^*$ reacts with O_2 to form reactive oxygen species (ROS), which further oxidize and degrade CIP(Cardoza et al., 2005; Gan et al., 2019; Ge et al., 2010; Lin et al., 2018). Therefore, Sorbic acid (HAD) was employed as an excited-state parent quenching agent to investigate its effects on direct photolysis. The addition of HAD

resulted in a notable reduction in the degradation effect of CIP in both conditions without and with Cu(II), with the degradation efficiency of CIP being inhibited by roughly 80% and 60%, respectively (**Fig. 3a**). It was determined that direct photolysis is the primary mode of degradation for CIP. Furthermore, •OH, $^1O_2$, $•O_2^-$, and e^- are all involved in the degradation of CIP (**Fig. 3a**). In the absence of Cu(II), DABCO demonstrated the strongest inhibitory effect. However, the contributions of •OH, $^1O_2$ and $•O_2^-$ were all increased in the presence of Cu(II), and •OH >$^1O_2$> $•O_2^-$ could be observed. This also indicates that Cu(II) enhances the involvement of ROS in the CIP photolysis process. The EPR results shown in **Fig. 3b** provide further evidence for this conclusion. They indicate that the signals of •OH and $•O_2^-$ in the CIP system are weaker in the absence of Cu(II) under visible light conditions. However, the signals of •OH and $•O_2^-$ are significantly amplified in the presence of Cu(II), with the intensity ratios being 1:2:2:1 and 1:1:1, respectively. This is also consistent with the results of our previous quenching experiments. Thus, Cu(II) enhances the action of •OH and $•O_2^-$ on CIP in the visible system, which in turn promotes the indirect photolysis of CIP.

To provide a clearer understanding of the influence of Cu(II) on the excited state of CIP, which was characterized by laser flash spectroscopy (**Fig. S4**). It was demonstrated that in the absence of Cu(II), CIP is more prone to the formation of excited triplet states, which subsequently absorb photons and undergo direct photolysis. With an increase in the Cu(II) concentration, the transient absorption values at the onset point decrease, indicating that Cu(II) reduces the generation of excited triplet states of CIP. Thus, the confirmation of the indirect photolysis of CIP facilitated by Cu(II) was further supported when paired with **Fig. 3a**.

Based on these results, the following rational reaction mechanism is proposed in this paper: CIP acts as a photosensitizer, whereby photons are absorbed, an electron of CIP can be promoted to the excited state ($^1CIP^*$) followed by intersystem crossing and generation of CIP triplet state ($^3CIP^*$) (Eq. (5))(Blázquez-Castro, 2017; Sciscenko et al., 2021). $^3CIP^*$ can produce degradation products when exposed to light (Eq. (7)). On the other hand, $^3CIP^*$ can also be quenched by molecular oxygen ($^3O_2$) via an energy transfer reaction, resulting in the formation of singlet oxygen ($^1O_2$) and a CIP ground state (Eq. (8)). Subsequent oxidation of CIP is facilitated by photogenerated $^1O_2$ (Eq. (9)). Furthermore, when Cu(II) is present, CIP and Cu(II) react to form complexes, which are then transformed into $^3CIP^*$-Cu(II) in the presence of light, leading to further deterioration (Eqs. (10)~(12))(Pan et al., 2018; Sciscenko et al., 2021; Xu

et al., 2023). It has been demonstrated that Cu(II) exists in a polyvalent state, which undergoes a Fenton-like reaction to generate ROS and promote the decomposition of pollutants(Dong et al., 2024; Xu et al., 2023; Yang et al., 2023). It can therefore be postulated that under light conditions, due to ligand to metal charge transfer (LMCT) between CIP and Cu(II), Cu(II) is converted to Cu(I), and CIP itself was oxidized to intermediate products (CIP-ip) (Eq. (13)) is generated. In the presence of oxygen, Cu(I) oxidation can produce $\bullet O_2^-$, species able to generate H_2O_2 by recombination. The presence of Cu(I) and H_2O_2 can undergo Fenton reaction leading to the formation of •OH. These two ROS can further oxidize CIP (Eqs. (14)~(18)).

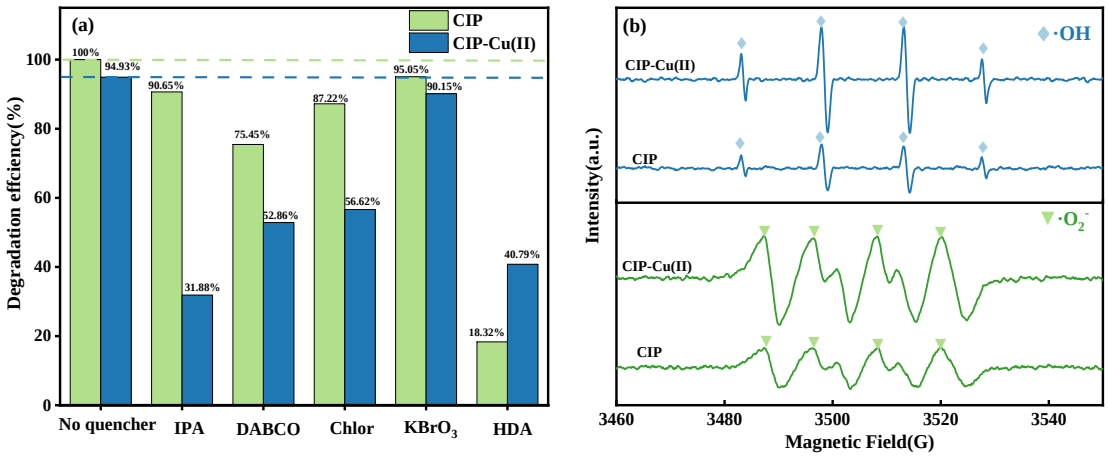

Fig. 3. (a) Quenching experiments on photodegradation of CIP in the presence and absence of Cu(II) in DI water, The reaction conditions: the molar ratio of CIP: Cu(II)= 1:40, pH=7, $[CIP]_0$=0.01 mM, $[Cu(II)]_0$ = 0.4 mM, [IPA]=0.2 M, [DABCO]=0.1 M, [Chlor]=0.05 M, $[KBrO_3]$=0.1 M, [HAD]=0.005 Mm, irradiation time = 8 h; (b) EPR spectra of CIP in DI water.

Equations

$$CIP \xrightarrow{hv} {}^1CIP^* \longrightarrow {}^3CIP^* \#(6)$$

$${}^3CIP^* \xrightarrow{hv} products\#(7)$$

$${}^3CIP^* + {}^3O_2 \longrightarrow {}^1O_2 + CIP\#(8)$$

$${}^1O_2 + CIP \longrightarrow products\#(9)$$

$$CIP + Cu(II) \longrightarrow CIP - Cu(II) \xrightarrow{hv} {}^3CIP^* - Cu(II)\#(10)$$

$${}^3CIP^* - Cu(II) \xrightarrow{hv} products - Cu(II)\#(11)$$

$${}^3CIP^* - Cu(II) + {}^3O_2 \longrightarrow {}^1O_2 + CIP - Cu(II) \longrightarrow products - Cu(II)\#(12)$$

$$CIP - Cu(II) \xrightarrow{hv} Cu(I) + CIP - ip \#(13)$$

$$Cu(I) + O_2 \longrightarrow Cu(II) + \bullet O_2^- \quad \#(14)$$

$$\bullet O_2^- + HO_2^\bullet + H_2O \longrightarrow H_2O_2 + O_2 + OH^- \#(15)$$

$$Cu(I) + H_2O_2 \longrightarrow Cu(II) + \bullet OH + OH^- \#(16)$$

$$\bullet OH + CIP - ip \longrightarrow products \#(17)$$

$$\bullet O_2^- + CIP - ip \longrightarrow products \#(18)$$

300

301 The Cu(II) transition metal ion significantly hindered the direct breakdown of CIP through a strong
302 interaction with it. To support this concept, Materials Studio software was utilized to calculate the highest
303 occupied molecular orbital (HOMO) for CIP and CIP-Cu(II) complex (**Fig. S1** and **Table 1**). The higher the
304 HOMO, the greater the ability to lose electrons at that position in theory, rendering it more prone to break
305 chemical bonds(Yan and Song, 2014). **Table 1** demonstrates a significant change in the HOMO values at
306 various places within the molecule after the formation of the Cu(II) complex. The atoms with greater HOMO
307 in the CIP compound are found primarily at the locations of 7C, 9C, 10C, 18N and 19N, which all belong to
308 the piperazine ring. However, the HOMO decreased substantially at positions 7C, 10C, 18N, and 19N within
309 the CIP-Cu (II) complex molecule, while they significantly increased at positions 4C,11C, 12C, 13C, 14C,
310 16C, 17C, 20N and 23O. The data indicate that the complexation of Cu (II) alters the HOMO values of the
311 atoms in the vicinity of the active center. The results demonstrated that the complexation of Cu(II) resulted
312 in the conversion of the active site of the main attack in the molecule from the piperazinyl ring to the 4C of
313 the C-F bond and the 11C, 12C, 13C and 20N of the pyridinyl ring, as well as the 14C and 16C of the
314 cyclopropyl group. In general, the formation of the Cu(II) complex results in a relative increase in the
315 HOMO value and the reactivity of the surrounding atoms. These positions are relatively active and are
316 therefore always the most vulnerable to be attacked by other species. Consequently, in the presence of Cu(II),
317 CIP is more susceptible to attack by active species such as $^1O_2$ and •OH, which promote indirect photolysis
318 of CIP.

319

320 **Table 1** The HOMO values of CIP and CIP-Cu(Ⅱ) complex calculated by using Materials Studio software

Number* (atom)	CIP	CIP-Cu(II)

1C	0.038742	0.056389
2C	0.194519	0.051214
3C	0.009127	0.016629
4C	0.051939	0.286497
5C	0.071624	0.082669
6C	0.051698	0.061348
7C	0.186228	0.028343
8C	0.014944	0.012244
9C	0.030984	0.005865
10C	0.179041	0.01115
11C	0.010785	0.185622
12C	0.007298	0.291456
13C	0.045888	0.203709
14C	0.005668	0.049936
15C	0.010068	0.086613
16C	0.008412	0.017468
17C	0.00254	0.290401
18N	0.42663	0.023663
19N	0.473719	0.021681
20N	0.030258	0.470046
21O	0.016178	0.022713
22O	0.028601	0.030754
23O	0.020306	0.234196
24F	0.102893	0.027234
43Cu	—	0.086137

321

322 In order to investigate the photodegradation mechanism effect of Cu(II) on CIP in DI water, the
323 photodegradation products of CIP were determined by UPLC-MS in two conditions (with and without

Cu(II)).

In the absence of Cu(II), the photodegradation of CIP was identified by the formation of three main products: P361, P290 and P245 (**Table S4**). The primary routes were inferred in **Fig. 4** based on our DFT findings and prior scholarly work(Li et al., 2021; Wei et al., 2015). The degradation of CIP is attributed to oxidative cleavage of the piperazine ring and photolytic defluorination. Indirect photolysis leads to the oxidative cleavage of the piperazine ring. Initially, the chemical bond between 9C and 10C in the piperazine ring in CIP is attacked by $^1O_2$, resulting in the opening of the piperazine ring. Subsequently, the ring undergoes further oxidation caused by •OH, resulting in the creation of a derivative containing a double aldehyde group, known as P361. In addition, $^1O_2$ oxidizes the 7C of the aldehyde group of P361, leading to the removal of a formaldehyde group and secondary amine nitrogen group leading to the formation of P290. Photolytic defluorination is a commonly seen occurrence that takes place during direct photolysis. It can be defined as the process by which CIP absorbs photons to form $^3CIP^*$ and is susceptible to photon attack. The continuous attack by light results in the complete oxidation of the side chain of the piperazine ring to solely the amine group(Agrawal et al., 2007). Subsequently, the molecule undergoes C-F bond breaking and further oxidation of 18N to form P245. The significance of direct and indirect photolysis in the photodegradation of CIP has been confirmed.

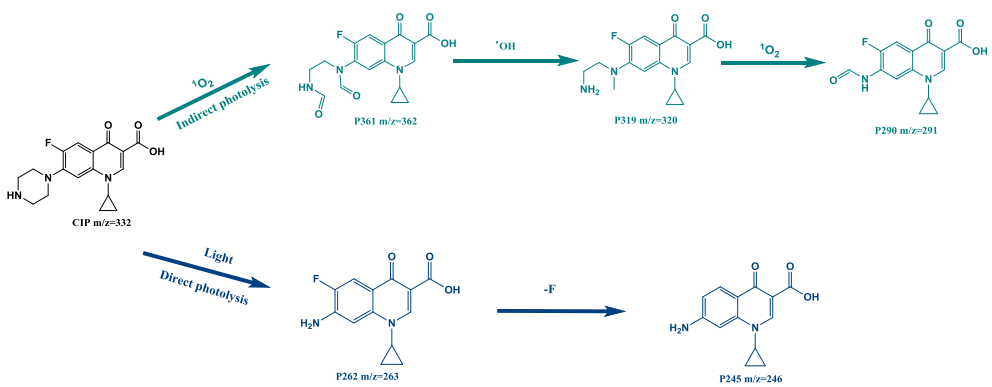

Fig. 4. Photodegradation pathway of CIP in DI water in the absence of Cu(II).

In the presence of Cu(II), three more degradation products of CIP, specifically P274, P292, and P314, were found in addition to the complexation product of CIP with Cu(II) and nine other degradation products (**Table S5**). The results of the product analysis demonstrated that direct and indirect photolysis also persisted

in the CIP-Cu(II) system. The inclusion of Cu(II) in the system led to a significant increase in the degradation pathways and degradation products, as depicted in **Fig. 5**. It was found that the piperazine ring of CIP also reacts is subjected to •OH and $•O_2^-$, resulting in the formation of a nitro product (P292). This is subsequently subjected to photolytic defluorination, leading to the generation of P274, as illustrated in the newly proposed pathway I(Cogan and Haas, 2008). Furthermore, CIP also undergoes direct photo-induced defluorination, which yields P314. This is then cleaved from the piperazine and piperazine ring of P314, resulting in the formation of P235, as depicted in the newly proposed pathway II(Lorenzo et al., 2008). In addition, the UPLC-MS analysis reveals the presence of Cu(II) complex products, including P290-Cu(II), 263-Cu(II), P245-Cu(II), P292-Cu(II), P274-Cu(II), and P314-Cu(II), in addition to the aforementioned products. It is hypothesized that intermediate products generated during the process of CIP degradation complex with Cu (II), resulting in the formation of P245-Cu(II) and P274-Cu(II) from P263-Cu(II) and P292-Cu(II), respectively, upon further light exposure.

Besides Path I and II, research has revealed that CIP can generate P287-Cu(II), P345-Cu(II), P334-Cu(II) and P316-Cu(II), as depicted in the newly proposed pathway III. (**Fig. 5**). The degradation pathways of CIP-Cu(II) complexes presumably include the following two pathways: 1. P313-Cu is the defluorination product of direct photolysis, which attacks 4C and then cleaves the piperazine ring to produce P287-Cu(II)(Cogan and Haas, 2008). 2. The 11C of the quinolone ring of the CIP-Cu(II) complex is attacked by •OH, leading to the formation of the hydroxylation product P345-Cu(II)(Taicheng An, 2010), which was then further oxidized in the presence of light and •OH, resulting in the decarbonylation to form P334-Cu(II) and P316-Cu(II)(Paul et al., 2010). In conclusion, the conversion of CIP in the presence of Cu(II) is a complex process involving several chemical reactions. The mentioned processes encompass hydroxylation, breaking of C-F bonds, cleavage of piperazine rings, and decarbonylation. The presence of Cu(II) caused the initiation of different degradation pathways and the modification of the degradation products of CIP photolysis.

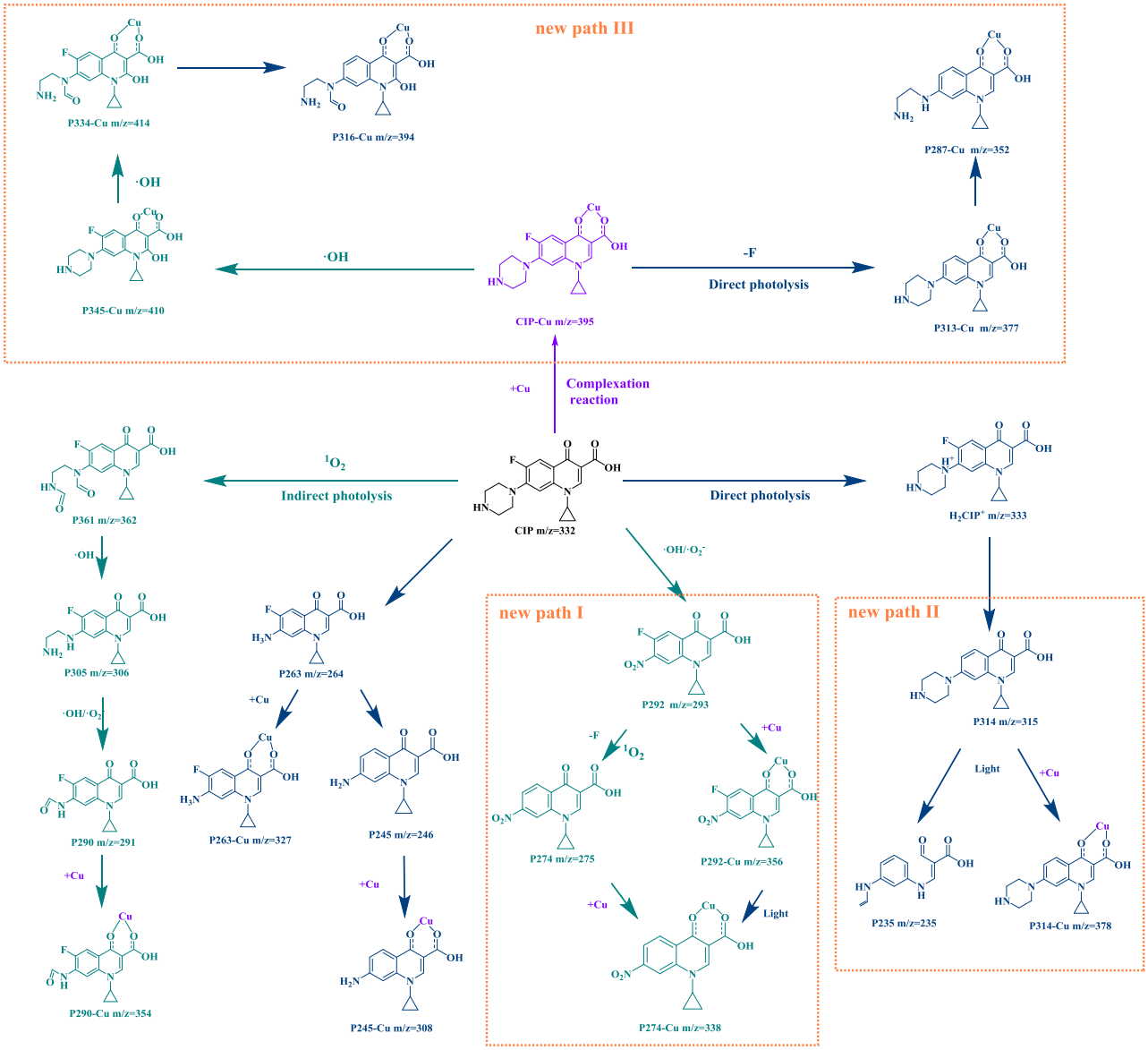

Fig. 5. Photodegradation pathway of CIP in DI water in the presence of Cu(II).

3.3.2 Exploring photodegradation of CIP in simulated mariculture water

The impact of simulated (SI) mariculture water on CIP photodegradation was explored in Section 3.2. However, the influence of Cu(II) on CIP photodegradation in SI water remains unclear. To gain further insight into the impact of Cu(II) in SI water on active species during CIP photodegradation, we conducted quenching and EPR experiments to provide a crucial foundation for understanding the transport and transformation of pollutants in real water matrix (**Fig. 6**). The results indicate that the photodegradation of CIP, regardless of the presence of Cu(II), was significantly inhibited only by the addition of DABCO, while the other quenchers had negligible effect on the degradation (**Fig. 6a**). This represents a significant divergence from the principal ROS in DI water. The quenching experiments also indicate that the

degradation efficiency of CIP does not decrease but rather increases to a certain extent when the other three quenching agents are added to the system, regardless of the presence or absence of Cu(II) in the degradation system. Furthermore, EPR spectra indicate that Cu(II) can facilitate the production of $^1O_2$, which aligns with the findings from our prior quenching experiments (**Fig. 6b**).

As demonstrated in Part 3.3.1, Cu(II) and CIP can act as the primary donors of ROS in DI water. However, the composition of SI water is intricate, and the presence of additional compounds can have a substantial impact on Cu(II) and CIP (Part 3.2). Therefore, the source of ROS in SI water requires further reasoning and validation. Previous studies have indicated that SI water contains a considerable quantity of dissolved organic matter (DOM), which can be a significant source of ROS in waters(Guo et al., 2023; Jieqiong Wang, 2018; McNeill and Canonica, 2016; Sharpless and Blough, 2014). The DOM is excited by absorbing a photon to form an excited single state of DOM ($^1DOM^*$), which is subsequently further excited to a triplet excited state ($^3DOM^*$) or a charge transfer state DOM ($DOM^{+\bullet/-\bullet}$) (Eq. (19)). Subsequently, $^3DOM^*$ or $DOM^{+\bullet/-\bullet}$, by quenching molecular oxygen, generates $^1O_2$ and $\bullet O_2^-$, respectively. Finally, with the participation of water and oxygen, $\bullet O_2^-$ reacts further to form •OH (Eqs. (20)~(23)). In addition to DOM, Cl^-, Br^-, HCO_3^-, and HNO_3^- in seawater also affect the photodegradation of organic pollutants(Guo et al., 2023; Li et al., 2016; Lin et al., 2013; Vione et al., 2009). Halogen ions and HCO_3^- are common scavengers of •OH, generating secondary radicals with low reactivity. The reaction mechanism is shown in Eqs. (24)~(26), where X represents halogen ions. Furthermore, studies have shown that the quantum yield of $^1O_2$ is around three orders of magnitude greater than that of •OH(Wan et al., 2019), rendering $^1O_2$ more efficient in SI water. In the presence of Cu(II), in addition to complexing with CIP in reactions such as Eqs. (9)~(14), free Cu(II) will react with $\bullet O_2^-$ to form dissolved oxygen and Cu(I) (Eq. (27)), while Cu(I) will also be oxidized to Cu(II) (Eq. (14))(Cai et al., 2020; Xing et al., 2018; Yuan et al., 2013). Based on the rate constants of 9.62×10^9 L $(mol\ s)^{-1}$ for the reaction of Cu(II) with $\bullet O_2^-$ and 0.48 L $(mol\ s)^{-1}$ for the reaction of Cu(I) with O_2, it can be inferred that most of the O_2 in the solution will serve as a substantial supplier of $^1O_2$ in SI water, leading to the degradation of CIP (Eq. (28)).

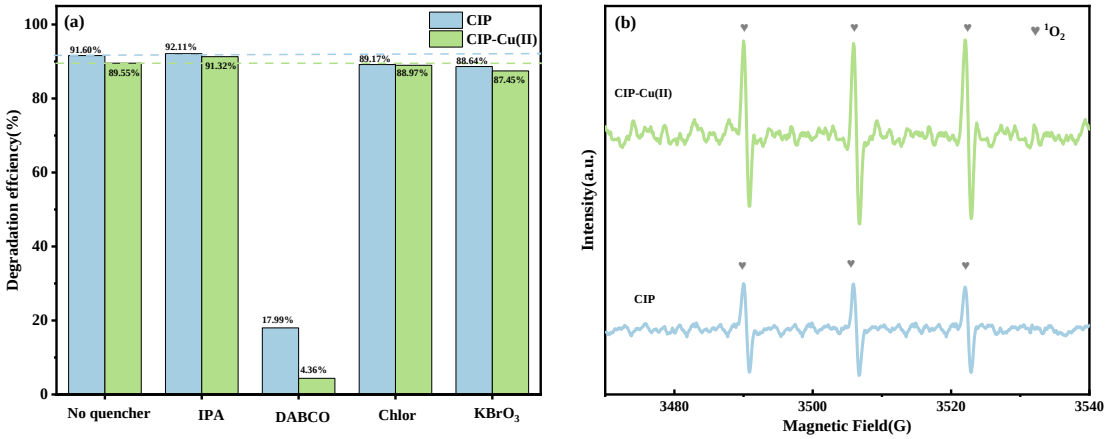

409

410 **Fig. 6.** (a) Quenching experiments on photodegradation of CIP in the presence and absence of Cu(II) in SI water, The

411 reaction conditions: the molar ratio of CIP: Cu(II) = 1:40, pH=7, $[CIP]_0$=0.01 mM, $[Cu(II)]_0$=0.4 mM, [IPA]=0.01 M,

412 [DABCO]=0.05 M, [Chlor]=0.05 M, $[KBrO_3]$=0.1 M, irradiation time = 8 h; (b) EPR spectra of CIP in SI water.

413 **Equations**

$$DOM \xrightarrow{\hbar v} {}^1DOM^* \rightarrow {}^3DOM^* \ or \ DOM^{+\bullet/-\bullet} \#(19)$$

$${}^3DOM^* + O_2 \longrightarrow DOM + {}^1O_2 \#(20)$$

$$DOM^{+\bullet/-\bullet} + O_2 \longrightarrow DOM^{+\bullet} + \bullet O_2^- \#(21)$$

$$DOM^{+\cdot} + \bullet O_2^- + 2H_2O \longrightarrow DOM + H_2O_2 + 2OH^- \#(22)$$

$$H_2O_2 + \bullet O_2^- \longrightarrow \cdot OH + H_2O + OH^- \#(23)$$

$$\bullet OH + X^- \rightleftharpoons XHO^{\bullet-} \#(24)$$

$$XHO^{\bullet-} \rightleftharpoons OH^- + X^{\bullet} \#(25)$$

$$HCO_3^-/CO_3^{2-} + \bullet OH \longrightarrow CO_3^{\bullet-} + H_2O/OH^- \#(26)$$

$$Cu(II) + \bullet O_2^- \longrightarrow O_2 + Cu(I) \#(27)$$

$${}^1O_2 + CIP/CIP - Cu(II) \longrightarrow products \#(28)$$

414

415 Degradation pathways of CIP in SI water might also be changed. LC-MS was applied to identify the

416 principal new products of CIP during photolysis (**Tables S6** and **S7**), and the most reasonable degradation

417 path were proposed in **Fig. 7** and **Fig. 8**. Clearly, in both water bodies, CIP undergoes piperazine ring

418 cleavage (at positions 9C and 10C) and defluorination (of the C-F bond) to generate hydroxylated,

419 nitroxylated, and defluorinated products. Nevertheless, in SI water, $^1O_2$ as the primary active substance

420 significantly alters the degradation products of CIP, as shown in Path A. The $^1O_2$ will attack the piperazine

ring in the CIP molecule, resulting in the formation of a product containing an O-O peroxy ring (P362)(Mella et al., 2001). Afterwards, the O-O peroxy ring can be further cleaved to form new products, including P335, P305, and P317, among others(Baena-Nogueras et al., 2017; Wan et al., 2019). This is markedly distinct from the degradation products observed in DI waters. Furthermore, the presence of Cu(II) also results in the formation of novel products, as illustrated in Path B. The 4C of the CIP-Cu(II) complex may create P329-Cu (II) complexes through substitution of fluor atoms by OH^- or H_2O. And then followed by the piperazine ring breakage to produce the P315-Cu(II) complex containing an amide group(Batchu et al., 2014). On the other hand, the formation of NOR-Cu(II) complexes is initiated by photon irradiation of the 14C and 16C of the cyclopropyl group, which is followed by the rupture of the piperazine ring via desethylation to form P294-Cu(II)(Guo et al., 2013, 2015; Lin et al., 2018).

Evidence showed that the photodegradation of CIP in the SI water will generate novel degradation products through new pathways, irrespective of the existence of Cu (II) in the system. Consequently, further research and study are required to gain a deeper understanding of this phenomenon. The presence of Cu(II) enhanced the role of $^1O_2$ in SI waters. However, Cu(II) was not the sole factor causing changes in the photodegradation of CIP in SI waters.

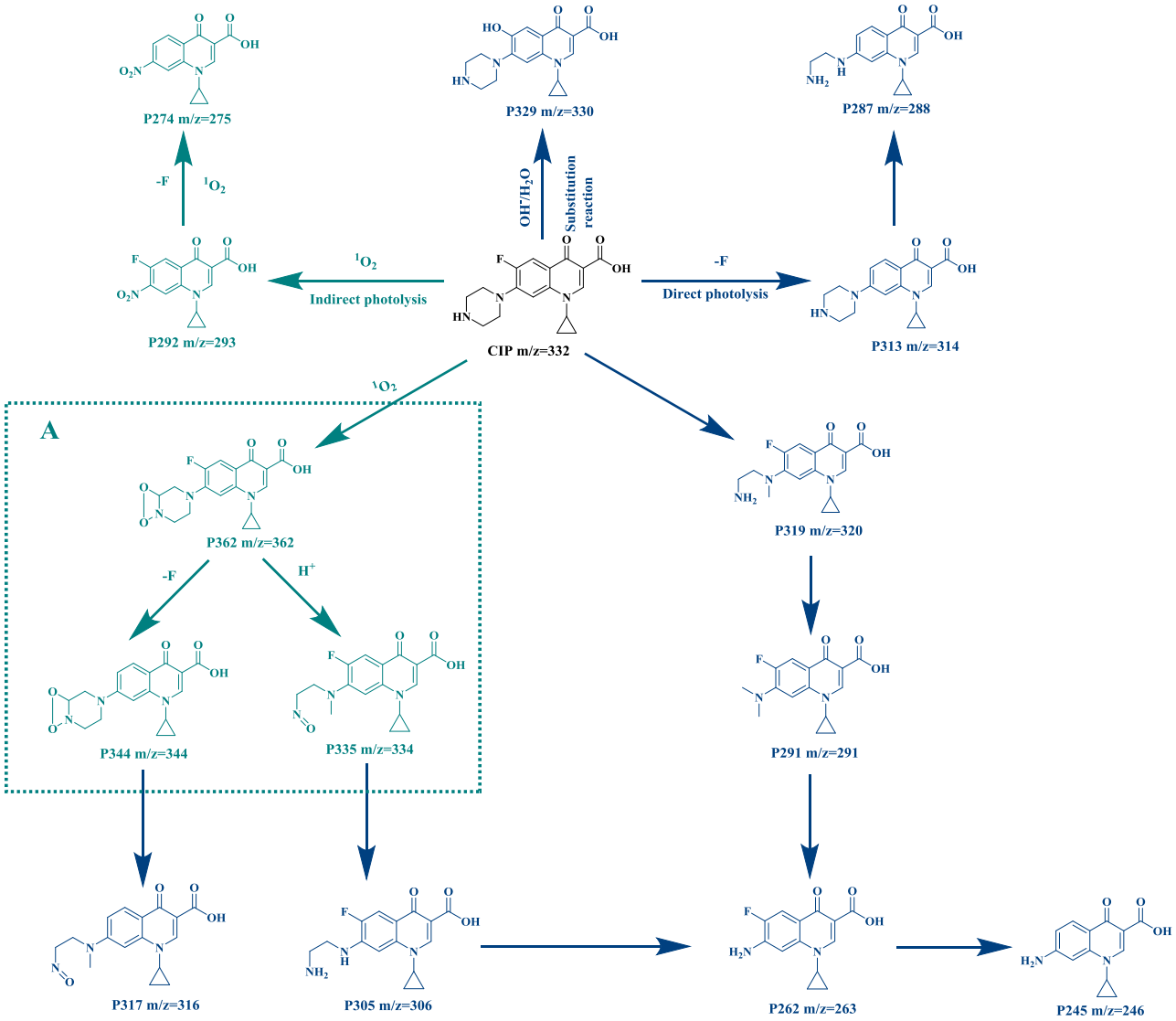

Fig. 7. Photodegradation pathway of CIP in SI water in the absence of Cu(II).

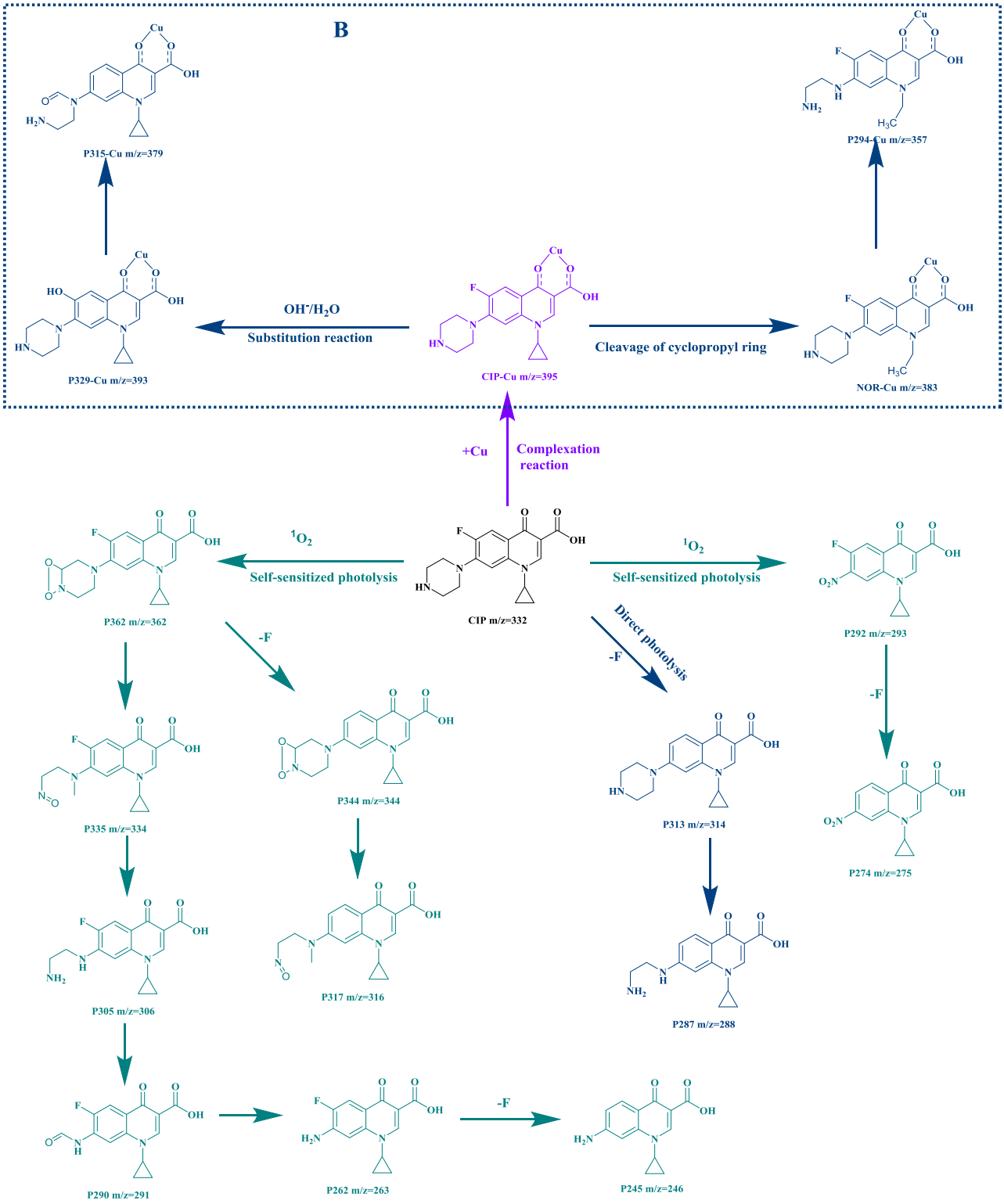

Fig. 8. Photodegradation pathway of CIP in SI water in the presence of Cu(II).

3.3.3 Toxicity analysis

Under the influence of Cu(II) and water background, ciprofloxacin photodegrades to produce a series of degradation products with different structures and chemical properties. Given the uncertain toxicity of the

intermediates, they may cause environmental re-contamination or pose a threat to human health. Therefore, it is crucial to predict and evaluate the toxicity of these intermediates. T.E.S.T software was used to evaluate a series of toxicity-related parameters of CIP and its by-products, including bioaccumulation factor, developmental toxicity, and mutagenicity (**Tables S8-S9 and Figs. 9(a-b)**)(Yang, 2021). It can be found that CIP and its intermediates are developmental toxicants (>0.5) under all circumstances, but the developmental toxicity of the intermediates decreases with the extension of reaction time. When only Cu(II) is present, P292 and P274 containing nitro groups show greater developmental toxicity. Under the combined action of Cu(II) and SI water, most of the intermediates of CIP show greater developmental toxicity than the parent. Except for P361, P314, P329, P313, P335, and P317, other intermediates of CIP showed mutagenicity negative (<0.5), indicating that during the photodegradation process, the mutagenicity of the intermediates began to decrease, which may be related to the changes in the piperazine ring.

In addition, the ECOSAR program was used to predict the acute and chronic toxicity of CIP and its intermediates to three aquatic organisms (i.e., fish, Daphnia, and algae) **(Tables S10-S11 and Figs. 9(c-d))**(Liu et al., 2024). In DI water, all three organisms were sensitive to chronic toxicity, among which P262/P263 and P245 showed "very toxic" to Daphnia. In addition, Cu(II) can significantly increase the toxicity of products containing nitro and amine groups such as P314, P292, P274, and P235 to Daphnia. Interestingly, the chronic toxicity of most intermediates of CIP in SI water to organisms is between "harmful" and "very toxic", and the acute toxicity is in the harmful range, which shows that the influence of the water environment on the production of CIP photodegradation products cannot be ignored. In short, Cu(II) and water matrix can change the degradation pathway of CIP and further affect the toxicity of the product. Unfortunately, there is no specific research method for the toxicity analysis of antibiotic-heavy metal complexes, so it is impossible to determine the environmental hazards caused by the complexes and conduct qualitative analysis. Therefore, more toxicity analysis studies on combined pollution are strongly recommended.

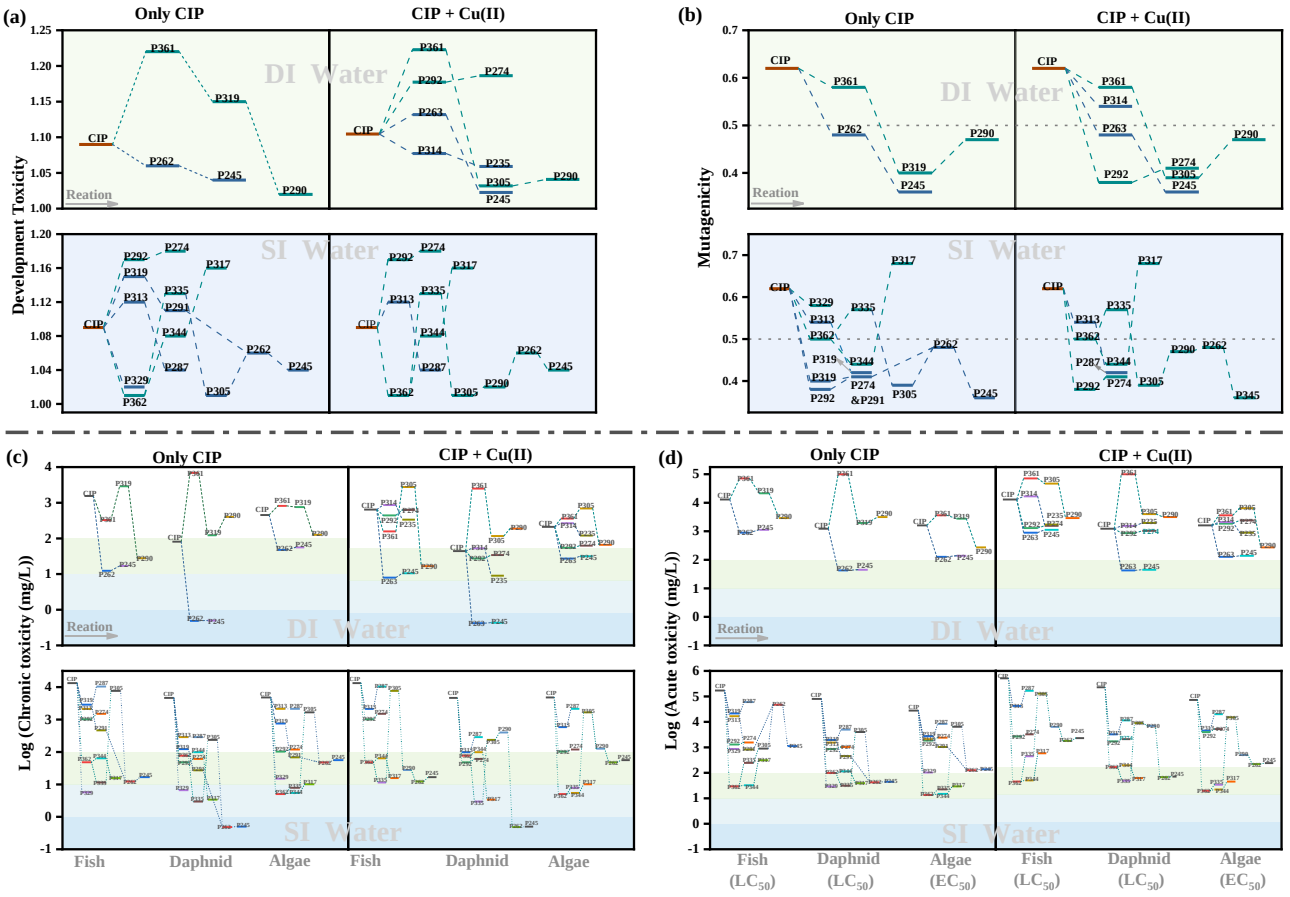

Figs. 9. Assessment of the developmental toxicity (a), mutagenicity (b), chronic toxicity (c), and acute toxicity(d) of CIP and its photolysis products was conducted using ECOSAR and T.E.S.T software.

4 conclusion

This research work presents the varying effects of Cu(II) on the degradation mechanism of CIP in different aqueous media. In the complexation study, CIP complexed with Cu(II) via the carboxyl group (COOH) in the molecular structure and the carbonyl group (C=O) in the keto group. Following this, investigations on the photodegradation of CIP in different water matrixs revealed that most metal cations hindered the photodegradation process, while anions and organic compounds had both promoting and inhibiting effects. Furthermore, Cu(II) plays multiple roles in the direct and indirect photolysis of CIP. In DI water, Cu(II) quenches the triplet excited state of CIP, thereby promoting the inhibition of direct photolysis. Additionally, Cu(II) facilitates the role of •OH and $•O_2^-$ in indirect photolysis through a Fenton-like reaction. In contrast, in SI waters, inorganic ions were observed to quench •OH and $•O_2^-$, whereas $^1O_2$ is mostly produced from the excited triplet state of organic matter and the indirect influence of Cu(II). Moreover, the degradation mechanism of CIP has experienced a substantial alteration. In DI water, the primary mechanism

responsible for CIP degradation is the cleavage of the piperazine ring and defluorination photolysis, which results in the formation of bis-aldehyde derivatives and amine-based products. When Cu(II) is present, CIP undergoes hydroxylation and decarbonylation, leading to the creation of hydroxylated and nitro compounds. These products subsequently form complexes with Cu(II). The degradation products and pathways of CIP are more numerous in SI water, where the aqueous matrix facilitates the formation of O-O peroxy ring intermediates from CIP, and Cu(II) promotes cyclopropyl cleavage of CIP to form new intermediates. Toxicity assessment showed that cleavage of the piperazine ring helped reduce the toxicity of the intermediates, but some products containing amine and nitro groups were more toxic than the parent molecule.

CRediT authorship contribution statement

Fang Zhong: Writing – original draft, Validation, Data curation, Software, Methodology. **Wenyu Huang:** Conceptualization, Resources, Supervision, Funding acquisition, Writing – review and editing. **Xiaoqing Feng:** Visualization, Investigation, Methodology. **Jia Zhang:** Formal analysis, Visualization. **Hongrui Zhang:** Validation. **Yiwu Dong:** Conceptualization. **Jingrao Li:** Validation, Visualization. **Liang Zou:** Validation, Resources. **Feishu Cao:** Resources, Funding acquisition. **Gilles MAILHOT:** Writing – review and editing.

Declaration of competing interest

The authors declare that they have no known competing financial interests or personal relationships that could have appeared to influence the work reported in this paper.

Acknowledgements

This study was funded by the Guangxi Science and Technology Major Program (grant number AA23073008), Hubei Key Laboratory of Water System Science for Sponge City Construction (Wuhan University) (grant number 2023-05) and Nanning Innovation and Entrepreneur Leading Talent Project (grant number 2021001).

Reference

Agrawal, N., Ray, R.S., Farooq, M., Pant, A.B., Hans, R.K., 2007. Photosensitizing Potential of Ciprofloxacin at Ambient Level of UV Radiation. Photochem. Photobiol. 83, 1226–1236. https://doi.org/10.1562/2006-10-12-RA-1059

Baena-Nogueras, R.M., González-Mazo, E., Lara-Martín, P.A., 2017. Photolysis of Antibiotics under Simulated Sunlight Irradiation: Identification of Photoproducts by High-Resolution Mass Spectrometry. Environ. Sci. Technol. 51, 3148–3156. https://doi.org/10.1021/acs.est.6b03038

Batchu, S.R., Panditi, V.R., O'Shea, K.E., Gardinali, P.R., 2014. Photodegradation of antibiotics under simulated solar radiation: Implications for their environmental fate. Sci. Total Environ. 470–471, 299–310. https://doi.org/10.1016/j.scitotenv.2013.09.057

Bel, E., 2009. Influence of pH on the sonolysis of ciprofloxacin: Biodegradability, ecotoxicity and antibiotic activity of its degradation products. Chemosphere 77, 291–295. https://doi.org/10.1016/j.chemosphere.2009.07.033

Blázquez-Castro, A., 2017. Direct 1O2 optical excitation: A tool for redox biology. Redox Biol. 13, 39–59. https://doi.org/10.1016/j.redox.2017.05.011

Cai, T., Bu, L., Wu, Y., Zhou, S., Shi, Z., 2020. Accelerated degradation of bisphenol A induced by the interaction of EGCG and Cu(II) in Cu(II)/EGCG/peroxymonosulfate process. Chem. Eng. J. 395, 125134. https://doi.org/10.1016/j.cej.2020.125134

Cardoza, L.A., Knapp, C.W., Larive, C.K., Belden, J.B., Lydy, M., Graham, D.W., 2005. Factors Affecting the Fate of Ciprofloxacin in Aquatic Field Systems. Water. Air. Soil Pollut. 161, 383–398. https://doi.org/10.1007/s11270-005-5550-6

Chang, P.-H., Li, Z., Jean, J.-S., Jiang, W.-T., Wu, Q., Kuo, C.-Y., Kraus, J., 2014. Desorption of tetracycline from montmorillonite by aluminum, calcium, and sodium: an indication of intercalation stability. Int. J. Environ. Sci. Technol. 11, 633–644. https://doi.org/10.1007/s13762-013-0215-2

Chen, H., Ma, L.Q., Gao, B., Gu, C., 2013. Influence of Cu and Ca cations on ciprofloxacin transport in saturated porous media. J. Hazard. Mater. 262, 805–811. https://doi.org/10.1016/j.jhazmat.2013.09.034

Cheng, D., Liu, H., E, Y., Liu, F., Lin, H., Liu, X., 2021. Effects of natural colloidal particles derived from a shallow lake on the photodegradation of ofloxacin and ciprofloxacin. Sci. Total Environ. 773, 145102. https://doi.org/10.1016/j.scitotenv.2021.145102

Chiron, S., Minero, C., Vione, D., 2006. Photodegradation Processes of the Antiepileptic Drug Carbamazepine, Relevant To Estuarine Waters. Environ. Sci. Technol. 40, 5977–5983. https://doi.org/10.1021/es060502y

Cogan, S., Haas, Y., 2008. Self-sensitized photo-oxidation of para-indenylidene–dihydropyridine derivatives. J. Photochem. Photobiol. Chem. 193, 25–32. https://doi.org/10.1016/j.jphotochem.2007.06.003

Cuprys, A., Pulicharla, R., Brar, S.K., Drogui, P., Verma, M., Surampalli, R.Y., 2018. Fluoroquinolones metal complexation and its environmental impacts. Coord. Chem. Rev. 376, 46–61. https://doi.org/10.1016/j.ccr.2018.05.019

Delley, B., 2000. From molecules to solids with the DMol3 approach. J. Chem. Phys. 113, 7756–7764. https://doi.org/10.1063/1.1316015

Deng, F., Zhang, D., Yang, L., Li, L., Lu, Y., Wang, J., Fan, Y., Zhu, Y., Li, X., Zhang, Y., 2022. Effects of antibiotics and heavy metals on denitrification in shallow eutrophic lakes. Chemosphere 291, 132948. https://doi.org/10.1016/j.chemosphere.2021.132948

Di Wu, 2012. Coadsorption of Cu and sulfamethoxazole on hydroxylized and graphitized carbon nanotubes. Sci. Total Environ. 427–428, 247–252. https://doi.org/10.1016/j.scitotenv.2012.03.039

Dong, Y., Huang, W., Liang, C., Gao, Y., Wei, Z., Meng, L., Zhong, F., Zhang, J., Zhou, L., Xu, J., 2024. Sulfamethazine degradation and copper transformation in Cu(II)/PMS system: In-depth investigation of the interaction between intermediates and copper. J. Water Process Eng. 58, 104929. https://doi.org/10.1016/j.jwpe.2024.104929

Duong, H.A., Pham, N.H., Nguyen, H.T., Hoang, T.T., Pham, H.V., Pham, V.C., Berg, M., Giger, W., Alder, A.C., 2008. Occurrence, fate and antibiotic resistance of fluoroquinolone antibacterials in hospital wastewaters in Hanoi, Vietnam. Chemosphere 72, 968–973. https://doi.org/10.1016/j.chemosphere.2008.03.009

Fan, Y., Chen, X., Chen, Z., Zhou, X., Lu, X., Liu, J., 2022. Pollution characteristics and source analysis of heavy metals in surface sediments of Luoyuan Bay, Fujian. Environ. Res. 203, 111911. https://doi.org/10.1016/j.envres.2021.111911

Gan, Y., Zhang, M., Xiong, J., Zhu, J., Li, W., Zhang, C., Cheng, G., 2019. Impact of Cu particles on adsorption and photocatalytic capability of mesoporous Cu@TiO_2 hybrid towards ciprofloxacin antibiotic removal. J. Taiwan Inst. Chem. Eng. 96, 229–242. https://doi.org/10.1016/j.jtice.2018.11.015

Garbin, J.R., Milori, D.M.B.P., Simões, M.L., da Silva, W.T.L., Neto, L.M., 2007. Influence of humic substances on the photolysis of aqueous pesticide residues. Chemosphere 66, 1692–1698. https://doi.org/10.1016/j.chemosphere.2006.07.017

Ge, L., Chen, J., Wei, X., Zhang, S., Qiao, X., Cai, X., Xie, Q., 2010. Aquatic Photochemistry of Fluoroquinolone Antibiotics: Kinetics, Pathways, and Multivariate Effects of Main Water Constituents. Environ. Sci. Technol. 44, 2400–2405. https://doi.org/10.1021/es902852v

Guo, H.-G., Gao, N.-Y., Chu, W.-H., Li, L., Zhang, Y.-J., Gu, J.-S., Gu, Y.-L., 2013. Photochemical degradation of ciprofloxacin in UV and UV/H2O2 process: kinetics, parameters, and products. Environ. Sci. Pollut. Res. 20, 3202–3213. https://doi.org/10.1007/s11356-012-1229-x

Guo, Y., Peng, B., Liao, J., 2024. Recent advances in the role of dissolved organic matter during antibiotics photodegradation in the aquatic environment. Sci. Total Environ. 916, 170101. https://doi.org/10.1016/j.scitotenv.2024.170101

Guo, Z., Kodikara, D., Albi, L.S., Hatano, Y., Chen, G., Yoshimura, C., Wang, J., 2023. Photodegradation of organic micropollutants in aquatic environment: Importance, factors and processes. Water Res. 231, 118236. https://doi.org/10.1016/j.watres.2022.118236

Guo, Z., Zhu, S., Zhao, Y., Cao, H., Liu, F., 2015. Radiolytic decomposition of ciprofloxacin using γ irradiation in aqueous solution. Environ. Sci. Pollut. Res. 22, 15772–15780. https://doi.org/10.1007/s11356-015-4715-0

He Z.W., Liu G.G., Liu H.J., Zhang N., Wang G., 2011. The effect of different nitrogen forms on the photo-degradation of ciprofloxacin in water. Acta Sci. Circumstantiae 31, 2409–2415. https://doi.org/10.13671/j.hjkxxb.2011.11.019

Hu, H., Chen, Y., Ye, J., Zhuang, L., Zhang, H., Ou, H., 2019. Degradation of ciprofloxacin by 185/254 nm vacuum ultraviolet: kinetics, mechanism and toxicology. Environ. Sci. Water Res.

Technol. 5, 564–576. https://doi.org/10.1039/C8EW00738A
Jieqiong Wang, 2018. DOM from mariculture ponds exhibits higher reactivity on photodegradation of sulfonamide antibiotics than from offshore seawaters. Water Res. 144, 365–372. https://doi.org/10.1016/j.watres.2018.07.043
Khurana, P., Pulicharla, R., Kaur Brar, S., 2021. Antibiotic-metal complexes in wastewaters: fate and treatment trajectory. Environ. Int. 157, 106863. https://doi.org/10.1016/j.envint.2021.106863
Li, Y., Qiao, X., Zhang, Y., Zhou, C., Xie, H., Chen, J., 2016. Effects of halide ions on photodegradation of sulfonamide antibiotics: Formation of halogenated intermediate. Water Res. 102, 405–412. https://doi.org/10.1016/j.watres.2016.06.054
Li, Z., Dong, D., Zhang, L., Li, Y., Guo, Z., 2022. Effect of fulvic acid concentration levels on the cleavage of piperazinyl and defluorination of ciprofloxacin photodegradation in ice. Environ. Pollut. 307, 119499. https://doi.org/10.1016/j.envpol.2022.119499
Li Z.L., Zhang G.L., Pan W.B., 2021. Preparation of Cu/Zn heterogeneous Fenton catalyst and its degradation effect of ciprofloxacin. Chin. J. Environ. Eng. 15, 806–816.
Lin, A.Y.-C., Wang, X.-H., Lee, W.-N., 2013. Phototransformation Determines the Fate of 5-Fluorouracil and Cyclophosphamide in Natural Surface Waters. Environ. Sci. Technol. 47, 4104–4112. https://doi.org/10.1021/es304976q
Lin, Y.-C., Hsiao, K.-W., Lin, A.Y.-C., 2018. Photolytic degradation of ciprofloxacin in solid and aqueous environments: kinetics, phototransformation pathways, and byproducts. Environ. Sci. Pollut. Res. 25, 2303–2312. https://doi.org/10.1007/s11356-017-0666-y
Liu, T., Li, N., Xiao, S., Chen, J., Ji, R., Shi, Y., Zhou, X., Zhang, Y., 2024. Revisiting iodide species transformation in peracetic acid oxidation: unexpected role of radicals in micropollutants decontamination and iodate formatio. Water Res. 265, 122270. https://doi.org/10.1016/j.watres.2024.122270
Lorenzo, F., Navaratnam, S., Edge, R., Allen, N.S., 2008. Primary Photophysical Properties of Moxifloxacin—A Fluoroquinolone Antibiotic. Photochem. Photobiol. 84, 1118–1125. https://doi.org/10.1111/j.1751-1097.2007.00269.x
Lulijwa, R., Rupia, E.J., Alfaro, A.C., 2020. Antibiotic use in aquaculture, policies and regulation, health and environmental risks: a review of the top 15 major producers. Rev. Aquac. 12, 640–663. https://doi.org/10.1111/raq.12344
McNeill, K., Canonica, S., 2016. Triplet state dissolved organic matter in aquatic photochemistry: reaction mechanisms, substrate scope, and photophysical properties. Environ. Sci. Process. Impacts 18, 1381–1399. https://doi.org/10.1039/C6EM00408C
Mella, M., Fasani, E., Albini, A., 2001. Photochemistry of 1-Cyclopropyl-6-fluoro-1,4-dihydro-4-oxo-7-(piperazin-1-yl) quinoline-3-carboxylic Acid (=Ciprofloxacin) in Aqueous Solutions. Helv. Chim. Acta 84, 2508–2519. https://doi.org/10.1002/1522-2675(20010919)84:9<2508::AID-HLCA2508>3.0.CO;2-Y
Monti, S., Sortino, S., Fasani, E., Albini, A., 2001. Multifaceted Photoreactivity of 6-Fluoro-7-amino quinolones from the Lowest Excited States in Aqueous Media: A Study by Nanosecond and Picosecond Spectroscopic Techniques. Chem. – Eur. J. 7, 2185–2196. https://doi.org/10.1002/1521-3765(20010518)7:10<2185::AID-CHEM2185>3.0.CO;2-U
Muthukumar, C., 2024. Synergistic photocatalytic degradation of ciprofloxacin under natural sunlight using hot dip galvanization and medical incineration waste residues. Environ. Pollut. 360, 12

4692. https://doi.org/10.1016/j.envpol.2024.124692
Pan, Y., Garg, S., Waite, T.D., Yang, X., 2018. Copper Inhibition of Triplet-Induced Reactions Involving Natural Organic Matter. Environ. Sci. Technol. 52, 2742–2750. https://doi.org/10.1021/acs.est.7b05655
Paul, T., Dodd, M.C., Strathmann, T.J., 2010. Photolytic and photocatalytic decomposition of aqueous ciprofloxacin: Transformation products and residual antibacterial activity. Water Res. 44, 3121–3132. https://doi.org/10.1016/j.watres.2010.03.002
Qin, Q., Wu, X., Chen, L., Jiang, Z., Xu, Y., 2018. Simultaneous removal of tetracycline and Cu(II) by adsorption and coadsorption using oxidized activated carbon. RSC Adv. 8, 1744–1752. https://doi.org/10.1039/C7RA12402C
Ramotowska, S., Wysocka, M., Brzeski, J., Chylewska, A., Makowski, M., 2020. A comprehensive approach to the analysis of antibiotic-metal complexe. TrAC Trends Anal. Chem. 123, 115771. https://doi.org/10.1016/j.trac.2019.115771
Rodríguez-López, L., Cela-Dablanca, R., Núñez-Delgado, A., Álvarez-Rodríguez, E., Fernández-Calviño, D., Arias-Estévez, M., 2021. Photodegradation of Ciprofloxacin, Clarithromycin and Trimethoprim: Influence of pH and Humic Acids. Molecules 26, 3080. https://doi.org/10.3390/molecules26113080
Schwarzenbach, R.P., Escher, B.I., Fenner, K., Hofstetter, T.B., Johnson, C.A., Von Gunten, U., Wehrli, B., 2006. The Challenge of Micropollutants in Aquatic Systems. Science 313, 1072–1077. https://doi.org/10.1126/science.1127291
Sciscenko, I., Arques, A., Varga, Z., Bouchonnet, S., Monfort, O., Brigante, M., Mailhot, G., 2021. Significant role of iron on the fate and photodegradation of enrofloxacin. Chemosphere 270, 129791. https://doi.org/10.1016/j.chemosphere.2021.129791
Sha, J., Li, L., An, Z., He, M., Yu, H., Wang, Y., Gao, B., Xu, S., 2022. Diametrically opposite effect of Cu^{2+} on sulfamerazine and ciprofloxacin adsorption-photodegradation in g-C_3N_4/visible light system: behavior and mechanism study. Chem. Eng. J. 428, 131065. https://doi.org/10.1016/j.cej.2021.131065
Sharpless, C.M., Blough, N.V., 2014. The importance of charge-transfer interactions in determining chromophoric dissolved organic matter (CDOM) optical and photochemical properties. Environ. Sci. Process. Impacts 16, 654–671. https://doi.org/10.1039/C3EM00573A
Silva, C.P., Louros, V., Silva, V., Otero, M., Lima, D.L.D., 2021. Antibiotics in Aquaculture Wastewater: Is It Feasible to Use a Photodegradation-Based Treatment for Their Removal? Toxics 9, 194. https://doi.org/10.3390/toxics9080194
Taicheng An, 2010. Kinetics and mechanism of advanced oxidation processes (AOPs) in degradation of ciprofloxacin in water. Appl. Catal. B Environ. 94, 288–294. https://doi.org/10.1016/j.apcatb.2009.12.002
Tan, L., Li, L., Ashbolt, N., Wang, X., Cui, Y., Zhu, X., Xu, Y., Yang, Y., Mao, D., Luo, Y., 2018. Arctic antibiotic resistance gene contamination, a result of anthropogenic activities and natural origin. Sci. Total Environ. 621, 1176–1184. https://doi.org/10.1016/j.scitotenv.2017.10.110
Tong, C., Zhuo, X., Guo, Y., 2011. Occurrence and Risk Assessment of Four Typical Fluoroquinolone Antibiotics in Raw and Treated Sewage and in Receiving Waters in Hangzhou, China. J. Agric. Food Chem. 59, 7303–7309. https://doi.org/10.1021/jf2013937

Trovó, A.G., Nogueira, R.F.P., Agüera, A., Sirtori, C., Fernández-Alba, A.R., 2009. Photodegradation of sulfamethoxazole in various aqueous media: Persistence, toxicity and photoproducts assessment. Chemosphere 77, 1292–1298. https://doi.org/10.1016/j.chemosphere.2009.09.065

Van Doorslaer, X., 2011. UV-A and UV-C induced photolytic and photocatalytic degradation of aqueous ciprofloxacin and moxifloxacin: Reaction kinetics and role of adsorption. Appl. Catal. B Environ. 101, 540–547. https://doi.org/10.1016/j.apcatb.2010.10.027

Vione, D., Feitosa-Felizzola, J., Minero, C., Chiron, S., 2009. Phototransformation of selected human-used macrolides in surface water: Kinetics, model predictions and degradation pathways. Water Res. 43, 1959–1967. https://doi.org/10.1016/j.watres.2009.01.027

Wan, D., Sharma, V.K., Liu, L., Zuo, Y., Chen, Y., 2019. Mechanistic Insight into the Effect of Metal Ions on Photogeneration of Reactive Species from Dissolved Organic Matter. Environ. Sci. Technol. 53, 5778–5786. https://doi.org/10.1021/acs.est.9b00538

Wang, A., Zhou, P., Tian, D., Zhang, H., Xiong, Z., Du, Y., He, C., Yuan, Y., Chen, T., Liu, Y., Lai, B., 2022. Enhanced oxidation of fluoroquinolones by visible light-induced peroxydisulfate: The significance of excited triplet state species. Appl. Catal. B Environ. 316, 121631. https://doi.org/10.1016/j.apcatb.2022.121631

Wang, Q., He, X., Xiong, H., Chen, Y., Huang, L., 2022. Structure, mechanism, and toxicity in antibiotics metal complexation: Recent advances and perspectives. Sci. Total Environ. 848, 157778. https://doi.org/10.1016/j.scitotenv.2022.157778

Wei, X., Chen, J., Xie, Q., Zhang, S., Li, Y., Zhang, Y., Xie, H., 2015. Photochemical behavior of antibiotics impacted by complexation effects of concomitant metals: a case for ciprofloxacin and Cu(II). Environ. Sci. Process. Impacts 17, 1220–1227. https://doi.org/10.1039/C5EM00204D

Wolters, A., Steffens, M., 2005. Photodegradation of Antibiotics on Soil Surfaces: Laboratory Studies on Sulfadiazine in an Ozone-Controlled Environment. Environ. Sci. Technol. 39, 6071–6078. https://doi.org/10.1021/es048264z

Wu, Q., Que, Z., Li, Z., Chen, S., Zhang, W., Yin, K., Hong, H., 2018. Photodegradation of ciprofloxacin adsorbed in the intracrystalline space of montmorillonite. J. Hazard. Mater. 359, 414–420. https://doi.org/10.1016/j.jhazmat.2018.07.041

Xing, G., Pham, A.N., Miller, C.J., Waite, T.D., 2018. pH-dependence of production of oxidants (Cu(III) and/or HO•) by copper-catalyzed decomposition of hydrogen peroxide under conditions typical of natural saline waters. Geochim. Cosmochim. Acta 232, 30–47. https://doi.org/10.1016/j.gca.2018.04.016

Xu, C., Feng, Y., Zhao, X.-X., Zhao, S., Wang, S.-G., Song, C., 2023. Mechanisms of Cu(II) enhancing photolysis of tetracycline under UV irradiation. Chem. Eng. J. 474, 145510. https://doi.org/10.1016/j.cej.2023.145510

Yan, S., Song, W., 2014. Photo-transformation of pharmaceutically active compounds in the aqueous environment: a review. Environ. Sci. Process. Impacts 16, 697–720. https://doi.org/10.1039/C3EM00502J

Yang, G., 2021. Molten salt-assisted synthesis of Ce_4O_7/Bi_4MoO_9 heterojunction photocatalysts for Photo-Fenton degradation of tetracycline: Enhanced mechanism, degradation pathway and products toxicity assessment. Chem. Eng. J. 425, 130689. https://doi.org/10.1016/j.cej.2021.130689

Yang, R., van den Berg, C.M.G., 2009. Metal Complexation by Humic Substances in Seawater. Env

iron. Sci. Technol. 43, 7192–7197. https://doi.org/10.1021/es900173w

Yang, Z., Sun, Y., Hou, Z., Yu, H., Li, M., Li, Yanwei, Li, Yude, Gao, B., Xu, S., 2023. Repeated fluctuation of Cu^{2+} concentration during photocatalytic purification of SMZ-Cu^{2+} combined pollution: Behavior, mechanism and application. J. Hazard. Mater. 447, 130768. https://doi.org/10.1016/j.jhazmat.2023.130768

Yu, Y., Wu, K., Xu, W., Chen, D., Fang, J., Zhu, X., Sun, J., Liang, Y., Hu, X., Li, R., Fang, Z., 2021. Adsorption-photocatalysis synergistic removal of contaminants under antibiotic and Cr(VI) coexistence environment using non-metal g-C3N4 based nanomaterial obtained by supramolecular self-assembly method. J. Hazard. Mater. 404, 124171. https://doi.org/10.1016/j.jhazmat.2020.124171

Yuan, X., Pham, A.N., Miller, C.J., Waite, T.D., 2013. Copper-Catalyzed Hydroquinone Oxidation and Associated Redox Cycling of Copper under Conditions Typical of Natural Saline Waters. Environ. Sci. Technol. 47, 8355–8364. https://doi.org/10.1021/es4014344